Journal of Arid Environments 66 (2006) 336–352

Journal of Arid Environments

www.elsevier.com/locate/jnlabr/yjare

Quantitative estimation of land cover structure in an arid region across the Israel–Egypt border using remote sensing data

Z. Qin[a,b,*], W. Li[a], J. Burgheimer[c], A. Karnieli[c]

[a]*Institute of Agro-Resources and Regional Planning, Chinese Academy of Agricultural Sciences, Beijing 100081, China*

[b]*International Institute for Earth System Sciences, Nanjing University, Nanjing 210093, China*

[c]*J. Blaustein Institute for Desert Research, Ben Gurion University of the Negev, Sede Boker Campus 84990, Israel*

Received 11 May 2004; received in revised form 1 November 2005; accepted 2 November 2005
Available online 5 January 2006

Abstract

The clearly visible border between the Israeli Negev and the Egyptian Sinai in remote sensing imagery is a very interesting phenomenon that has long been studied. The widely accepted explanation to this observation is a viewpoint of anthropogenic impacts on the arid environmental ecosystem across the border. In order to examine the validity of this viewpoint, three methods were employed in this study to determine the quantitative structure of main land cover patterns (biogenic crust, bare sand, vegetation and playa) in the arid region: field observation, measurement on aerial photograph, and analysis of vegetation cover changes on Landsat Thematic Mapper (TM) and SPOT images. Field observation on the Israeli side indicated that vegetation covers ~16% of the ground, biogenic crust ~69%, sand ~12% and playa 3%. Evidence from aerial photograph supported a sharp contrast of vegetation cover across the border, with ~17% on the Israeli side and ~6% on the Egyptian side. Analysis of the available TM/SPOT images indicated a high vibration of seasonal vegetation changes in the region. The Israeli side had a vegetation cover rate ranging from above 18% in the growing season and below 5% in the dry months. The rate on the Egyptian side changes from less than 2% in the dry season to ~5% in the growing season. Therefore, it is reasonable to estimate surface composition structure of the region as follows: vegetation, biogenic crust, bare sand and playa account for 5–18%, 71–84%, 7.5% and 3.5%, respectively, on the Israeli side, and 2–5%, 12.5%, 79–82% and 3.5% on the Egyptian side, depending on the season.

*Corresponding author. Institute of Agro-Resources and Regional Planning, Chinese Academy of Agricultural Sciences, Beijing 100081, China. Tel.: +86 10 6897 5171.

E-mail addresses: qinzh@caas.net.cn (Z. Qin), karnieli@bgumail.bgu.ac.il (A. Karnieli).

0140-1963/$ - see front matter
doi:10.1016/j.jaridenv.2005.11.003

This estimate of land cover structure has been successfully used to model land surface temperature differences across the border, in order to understand arid ecosystem evolution in the region.

Keywords: Vegetation; Biogenic crust; Sand dune; Surface temperature; Landsat TM; SPOT

1. Introduction

The clear visibility of the Israel–Egypt political border in the arid environment of Negev–Sinai Peninsula (Fig. 1) has long been reported and studied (Otterman 1974, 1977, 1981; Warren and Harrison, 1984; Tsoar and Møller, 1986). The border region is mainly composed of linear sand dunes stretching from the Egyptian Sinai into the Israeli Negev with identical lithological unit and geomorphorlogical landscape. Formation of the sand dunes is mainly attributed to deposition of fine sand and dust transported from the northern African desert by strong winds. On remote sensing images (such as Fig. 1) of visible channels, this arid region is characterized by a sharp contrast between bright reflectance from the Egyptian side (Sinai) and dark one from the Israeli side (Negev) (Pinker and Karnieli, 1995; Tsoar and Karnieli, 1996; Qin et al., 2001). The contrast has been interpreted as being caused by different land cover structures under different land use policies in the arid environmental ecosystem crossing the border (Otterman, 1974, 1977, 1981; Warren and Harrison, 1984; Tsoar and Møller, 1986). The Egyptian side has few

Fig. 1. Landsat TM image of the arid region across the Israel–Egypt border, composed of bands 4, 3 and 2 as RGB, acquired on March 29, 1995. The sand dunes can be clearly seen on the image of the arid region. N1 is the Nizzana settlement, and N2 the Nizzana Research Site. The inserted box indicates the geographical location of the SPOT images used for the study.

vegetation cover and prevalent bare sand surface. The Israeli side is, in contrast, dominated by shrubs and inactive sand surface fixed by biogenic crust, dubbed microbial crust (Kidron and Yair, 1997). The thin biogenic crust (usually <5 mm) is an overwhelming surface pattern in the western Negev and is scarce in the northern Sinai due to intensive anthropogenic activities on the Egyptian side of the border (Tsoar and Møller, 1986). It is believed that the relatively low spectral reflectance of biogenic crust and desert plants vs. bare sand is the main contribution to the high visibility of the political border in remote sensing imagery (Karnieli, 1997). A similar spectral contrast is also observed in the desert environment along the USA–Mexico border (Bahre and Bradbury, 1978; Balling, 1989; Balling et al., 1998). The USA side is darker because of its denser vegetation cover. The Mexican side is brighter because of its prevalent bare surface, as a result of severe overgrazing (Balling et al., 1998).

Having relatively dense vegetation cover, the Israeli side should be cooler than the Egyptian side. This has been the case in the arid region across the USA–Mexico border (Balling, 1989). However, an opposite thermal change is observed on daytime images of the Israel–Egypt border region. Land surface temperature (LST) is clearly higher on the Israeli side than on the Egyptian side (Qin et al., 2001, 2002a). This phenomenon does not only occur on particular days. It can be observed on almost every day of the year, except for a handful of days when the ground is very wet and cool. Considering the denser vegetation cover on the Israeli side, we can term this temperature difference across the border as an anomalous phenomenon. The sharp contrast of LST across the border does not generally appear on nighttime thermal images (Qin et al., 2002a). An explanation was suggested in our studies, based on deliberate examination of remote sensing analysis (Qin et al., 2002a), micrometeorological modeling (Qin et al., 2002b, c), and ground temperature measurement (Qin et al., 2005). This thermal anomaly was found to be mainly due to the combined effects of different land cover structures and their different thermal processes governed by different physical properties on both sides. The obvious differences in biogenic crust cover and bare sand between the two sides, as well as the temperature differences between the two prevelant surfaces (biogenic crust and bare sand) due to their differences in albedo, overcome the weak cooling contributed by vegetation cover on the Israeli sides (Qin et al., 2002a, b). As a result, the Israeli side is hotter than the Egyptian side.

Considering the identical lithological units and geomorphological patterns, the sharp spectral contrast across the Israel–Egypt border must be caused by the differences in the magnitude of land cover structure of various patterns. Thus, estimation of land cover structure in the region is critical for understanding the generation of a visible border in both the visible and thermal channels of remote sensing images. To date, however, actual land cover structure has never been quantitatively determined although several studies have mentioned the differences, particularly in vegetation density across the border. As indicated in several studies, such as Tsoar and Møller (1986) and Karnieli (1997), the region can be seen to be composed of four main land cover patterns: biogenic crust, bare sand, desert vegetation, and playa. It is the differences in land cover structure that lead to the existence of the sharp spectral contrast between the two sides of the border. Therefore, knowing the quantitative composition of land cover patterns is extremely important in suggesting an acceptable explanation for this interesting phenomenon. Nevertheless, accurate percentages of each surface pattern have never been reported, even though several studies (Otterman, 1974, 1977, 1981; Tsoar and Møller, 1986; Karnieli, 1997) have noted that there is more vegetation cover on the Israeli side than on the Egyptian one.

Kidron and Yair (1997) arbitrarily guessed 10–40% vegetation cover, Otterman and Robinove (1982) 20%, on the Israeli side. The plant communities at the Nizzana Research Site (Fig. 1) were investigated by Tielböger (1997), who reported that the percentage of plant cover at that site differed from community to community, i.e., 1.9% for *Anabasis articulata* to 32.1% for *Noaea mucronata–Artemisia monosperma* (Tielböger, 1997). The exact percentages of other surface patterns, such as biogenic crust and bare sand, have never been reported.

In this paper, we intend to estimate the percentages of the main land cover patterns in this arid region. Three methods were employed for the estimation: field observation, measurement on aerial photograph, and analysis of available Landsat TM and SPOT images. The average percentage of each land cover pattern is determined on the basis of the data culled from the methods. Spatial variation and seasonal changes of vegetation cover across the border are also examined.

2. The study region and relevant research

The study region is located in the northwestern part of the Israeli–Egypt political border. It covers an area of about $30 \times 40\,km^2$ (30 km along the border and a width of ~20 km on each side). Geomorphological patterns in the arid region are mainly linear sand dunes and interdune valleys stretching from the Egyptian side into Israel. Fine sand with a diameter of 0.05–0.1 mm (Gerson et al., 1985) is the main soil constituent in the region though silt and clay also account for some percentages ($<5\%$), especially on the Israeli side where a thin biogenic crust covers most of the surface. Average annual rainfall in the arid region is ~95 mm (Kidron and Yair, 1997). The rainy season is usually from November to April of next year.

On the Egyptian side, the arid region is under intensive use by Bedouin nomads for grazing and cropping. High plants (shrubs) have been subjected to severe gathering for firewood (Tsoar and Møller, 1986). In contrast to free use on the Egyptian side, the region on the Israeli side (Negev) has been managed under strict conservation policies. Limited anthropogenic activities have led to the establishment of vegetation (shrubs and annuals) and biogenic crust. The crust is mainly composed of clay, lichen, fungi and other microphytes, especially chlorophyll-containing cyanobacteria.

Land use differences between Israel and Egypt have a pronounced effect on remote sensing imagery, where a sharp spectral contrast across the border can be clearly seen. This contrast has attracted much scientific inquiry over decades (Otterman, 1974; Tsoar and Møller, 1986; Danin, 1991; Karnieli and Tsoar, 1995; Tsoar and Karnieli, 1996; Karnieli, 1997). Relatively higher reflectance on the Egyptian side is believed to be the direct result of severe anthropogenic impacts by the Sinai Bedouin, including overgrazing and firewood gathering (Tsoar and Møller, 1986).

Otterman (1974) observed the contrast in the first Landsat image taken in 1972 and pointed out that semi-dormant desert fringe plants strongly reduce the albedo of sandy terrain. Karnieli and Tsoar (1995) suggested a different interpretation for the spectral contrast: the biogenic crust covering most of the Israeli side contributes a darker tone to remote sensing imagery. Anthropogenic activities on the Egyptian side that prevent the establishment of this crust contribute to the brighter tone. Therefore, it was concluded that the well-known contrast between the Sinai and the Negev in remote sensing imagery is not a direct result of vegetation cover differences but caused by the almost complete cover of

biogenic crust in the Israeli Negev and the scarcity of that crust in the Egyptian Sinai (Karnieli and Tsoar, 1995). Tsoar and Karnieli (1996) studied the change in spectral reflectance values in remote sensing. On the Israeli side, increment in biogenic crust generally comes together with increase in vegetation cover. The sand dunes are low and stable with high percentage of biogenic crust in the interdunes. The crust is developed by microphytes from fines (silt and clay). The region is covered with dense carpets of wilted annuals, which have a reflectance that is lower than that of the crusted area but higher than that of *artemisia* shrub (Tsoar and Karnieli, 1996).

The contrast across the border is also observed in the thermal range of the electromagnetic spectrum. Otterman and Tucker (1985) related this thermal contrast to severe overgrazing and other anthropogenic pressures on the Egyptian side. The mechanism leading to the thermal contrast has been simulated using a micrometeorological model on the basis of surface energy balance (Qin et al., 2002b, c). According to the simulation results, Qin et al. (2002b) suggested that the thermal contrast is due mainly to the differences in land cover structure, especially biogenic crust vs. bare sand across the border. The thermal anomaly has been thoroughly examined from the viewpoint of remote sensing analysis (Qin et al., 2002a). Combining ground truth measurement of surface temperature with determination of emissivity, Qin et al. (2005) proposed an approach on the basis of Stefan–Boltzman radiance law to simulate the average LST on both sides under various possible conditions. Simulation using the land cover structure estimated in the study successfully explained the observed LST difference, which could be attributed to the combined effects of the differences in land cover patterns and their different thermal properties on each side of the border (Qin et al., 2005). LST difference between the two sides appears to be obvious when surface temperature is above 30 °C, while the difference disappears when it is ~25 °C (Qin et al., 2005). This is exactly identical to the actual thermal phenomenon observed in remote sensing images of the region (Qin et al., 2002a). During daytime, surface temperature in the region generally reaches to 40–50 °C, leading to significant LST difference between the two sides. During nighttime, surface temperature in the region is usually ~25 °C, leading to no LST difference across the border (Qin et al., 2005). Therefore, the quantitative estimation of land cover structure in the study is part of a series of investigations into the thermal differences. Since land cover estimation is a very important step in remote sensing analysis of the earth's resources, especially in landscape ecological modeling and environmental monitoring, quantitative estimation of land cover structure in the region may also have potiental applications for relevant studies, such as understanding the different surface processes in terms of arid environment, ecology, geomorphology, sand movement, and so on.

3. Methods for determining the land cover structure

Three methods were used in this study to quantitatively determine the percentages of main land cover patterns in the region: field obervation, measurement on an aerial photograph with high spatial resolution, and analysis of Landsat TM and SPOT images for vegetation estimation.

3.1. Field observation

The field observation was performed at the Nizzana Research Site (Fig. 1) in the Israeli Negev. Primary purpose of the observation was to determine the percent vegetation cover

Table 1
Field observation at the Nizzana Research Site

Plot	Location	Total area (m^2)	Total shrub number	Shrub number sampled	Average diameter (m)	Shrub area (m^2)
1	Interdune	1330	198	27	1.06	175.2
2	Interdune	780	121	28	1.27	152.3
3	Bottom slope	740	168	30	1.05	146.3
4	Middle slope	330	42	15	1.09	44.5
5	Top dune	671	37	9	0.75	75.9
Total samples		566	3851	109	1.09	594.3

Note: Plots 5 has 7 big shrub patches with a total area of 62.5 m^2. Thus, its total area is equal to the area of 30 normal shrubs plus that of the big shrub patches.

on the Israeli side. Five rectangular plots of various sizes (300–1300 m^2, see Table 1) were selected for the observation. First, the area of each plot was measured and the total number of shrubs counted. Then, we randomly selected shrubs to measure their diameter for statistical analysis: measuring all of the shrubs in the plot would have been unnecessarily time-consuming and laborious. Finally, we calculated the average shrub diameter and estimated the total vegetation area based on the assumption that desert shrubs' canopies approximate a circular shape. The percentage of vegetation cover was computed as total vegetation area divided by total plot area. Since small shrubs did not fully cover the land and only those big shrubs (usually with a diameter of >1.5 m) were able to provide a thick dense canopy that might completely cover the ground, we only counted those shrubs of moderate size (diameter >0.5 m) as vegetation and neglected those with small diameter (<0.5 m). These sampling criteria were expected to compensate for some of the errors that may otherwise have arisen in the measurement.

The five sampling plots were distributed as follows: two plots in the interdune valleys, one at the foot of dune slope, one in the middle of the slope, and one at the top. The surface of the sampled plots was mainly constituted of biogenic crust mixed with vegetation (mainly shrubs) except the one at the top, which had land cover structure of bare sand mixed with vegetation. The sampling process and results from the field observation are shown in Tables 1 and 2, respectively.

3.2. Measurement on an aerial photograph

The aerial photograph used for the deliberate measurement is shown in Fig. 2. The photograph was acquired on May 22, 1993 by a camera with color film at a flight altitude of ~1000 m under clear sky. It thus has three channels in the visible range. The photograph covers both sides of the region, with an area of 1285×1390 m^2, though the Egyptian part is only ~400 m in width. The geographical location of the photograph is the same as the field observation: the Nizzana Research Site (see Fig. 1). The spatial resolution is high enough to clearly distinguish the shrub canopies from their surrounding background.

The methodology used to measure land cover patterns in the photograph included making subset images (dividing original photograph into two subsets: Israel and Egypt) and making measurement on the subsets. The subsets were created so that separate measurements could be conducted on each side for comparison of their land cover

Table 2
Land cover rates from the field observation

Plot	Location	Area (m^2)			Percentage (%)	
		Total	Shrub	Crust	Shrub	Crust
1	Interdune	1330	175.2	1154.8	13.2	86.8
2	Interdune	780	152.3	627.8	19.5	80.5
3	Bottom slope	740	146.3	593.7	19.8	80.2
4	Middle slope	330	44.5	285.5	14.8	85.2
5	Top dune	671	75.9	595.1(S)	11.3	88.7 (S)
Total samples		3851	594.3	2661.7	15.4	69.1

Note: Values followed by (S) refer to bare sand.

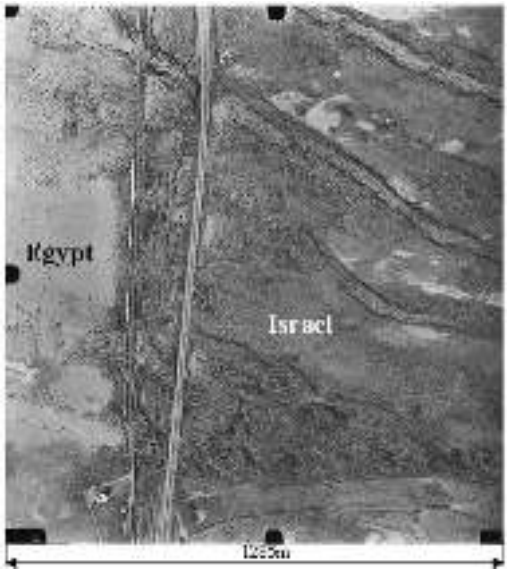

Fig. 2. Aerial photograph of the Nizzana Research site, acquired on May 22,1993 with color camera at altitude of ~1000 m. Two border highways are clearly seen. The dark dots are mainly shrub canopies. The bright plots are playa. The Egyptian side is dominated by bare sand and the Israeli side by biogenic crust.

differences. Usually, land cover patterns on remote sensing imagery are measured using the classification function of image analysers, such as ERDAS Imagine. We intended to classify the subsets into four basic patterns: vegetation, biogenic crust, bare sand and playa. Thus, our first choice was to use supervised classification with training points for the four patterns. The classification with several grouping methods did not give the expected result. There were always some misclassifications among the four patterns when using all three channels. It was really difficult to distinguish the patterns of playa and biogenic crust from bare sand due to the similarity in their pixel digital number (DN) values. Unsupervised classification was also unable to yield in a satisfactory result for quantitative estimation of the surface patterns. Thus, we decided to first classify the shrubs separately

from the other patterns on the channels, using the distinct differences in their DN values. Then, we used image interpretation methods to identify the other three patterns.

Since vegetation absorbs most incoming light at visible wavelengths, pixels with low DN values are usually desert shrub canopies in the photograph. Examination of some typical shrub canopies indicated that most of their pixels have a DN value of <65 and only a few on the edge have DN values higher than 65 but less than 80. Considering the possible error resulting from effects of leaf density and shrub debris, we decided to classify pixels with DN $\leqslant 60$ in channel 1 as vegetation. We also tried to distinguish other surface patterns in this way, but the overlap in their DN values made it impossible. For biogenic crust, most pixels have DN values ranging from 70 to 180, and for sand and playa, the values range from 120 to 255. Therefore, the numerical classification based on DN values did not enable us to successfully distinguish these two patterns. Instead, image interpretation method had to be applied. The spatial distribution of biogenic crust, bare sand and playa is very obvious in the images. Thus, we enlarged the images and drew polygons of the three patterns for area measurement. Some plots did not show a pure surface pattern, but a mixture with shrubs. This was especially true on biogenic crust where various shrubs were rampant. Some sand dunes also had various shrubs on their surface. This complicated the measurement because we had to subtract vegetation cover from the area.

On the Egyptian side, the ground is mainly covered with bare sand. So we decided to measure the relatively small plots of mixing biogenic crust with shrubs and playa with shrubs. The area of bare sand could then be gotten by subtracting the areas of vegetation, biogenic crust and playa from the total. The Egypt subset has 7 plots of biogenic crust mixed with vegetation and 2 playa plots with vegetation. The ground on the Israeli side was dominated by biogenic crust, but mixed with shrubs. Only a small part of the Israeli subset was covered with bare sand and playa (Fig. 2). Thus, we first measured the areas of the bare sand and playa plots. Then we termed the rest as biogenic crust mixture.

3.3. Analysis of vegetation cover rate on Landsat TM and SPOT images

Landsat TM and SPOT images have been extensively used for various studies of land cover mapping (Cihlar, 2000) due to their high spatial resolution (pixel size is $30\,m^2$ for TM and $10\,m^2$ for SPOT under the nadir). In this study, we had 6 TM images and 20 SPOT images for vegetation cover mapping in the arid region. These images were acquired over various periods and are therefore very suitable for comparing seasonal vegetation changes on each side. The TM images were acquired mainly in the mid-1990s and the SPOT images more recent (i.e. 2001–2003). Fig. 1 is a TM image acquired on March 29, 1995, illustrating the spatial differences in land cover structure across the border. The inserted box in this figure indicates the geographical location of the SPOT images: the area around the Nizzana Research Site.

Vegetation mapping from remote sensing images is theoretically based on the spectral characteristics of green vegetation. Normalized difference of vegetation index ($NDVI$) has been widely used for vegetation mapping. The index is computed from TM and SPOT images using the following formula:

$$NDVI = (IR - R)/(IR + R), \tag{1}$$

where IR and R represent infrared and red bands, respectively (bands 4 and 3, respectively, for TM, and bands 2 and 1 for SPOT). Because vegetation has very high reflectance in the

infrared wavelength and low in the red wavelength, the higher *NDVI* value, the more vegetation cover there is on the ground. However, this index does not directly indicate vegetation cover rate. Actually, because pixels of TM/SPOT images are larger than any single canopy of plants in the arid region, *NDVI* on the pixel scale may include signal from both the vegetation canopy and the background surface. In our case, the background may be biogenic crust, bare sand and playa. However, one can expect a maximum *NDVI* value for a fully vegetated canopy covering the ground and a minimum *NDVI* value for a pure background surface where there is no vegetation cover. *NDVI* values between the maximum and minimum then represent some fraction of the vegetation cover. According to this principle, vegetation cover rate (*VR*) can be calculated from *NDVI* as follows (Kerr et al., 1992):

$$VR = (NDVI - NDVI_b)/(NDVI_v - NDVI_b), \quad (2)$$

where $NDVI_v$ is the maximum *NDVI*, i.e., that of a fully vegetated surface, and $NDVI_b$ is the minimum *NDVI*, i.e., that of a pure background surface without vegetation. Thus, the accuracy of using *NDVI* to determine vegetation cover depends on the two important coefficients: $NDVI_v$ and $NDVI_b$.

Usually, $NDVI_v$ is above 0.70 for green leaves of healthy plants. In our arid region, vegetation cover was defined as a canopy of various shrubs, which do not fully cover the surface when viewed from the nadir. We used our experimental *NDVI* of *artemisia* (a typical shrub in the region) canopy measured in the field as $NDVI_v$, ~0.61 on average. The biogenic crust is mainly cyanobacterium crust in the region. According to the spectra presented in Karnieli (1997), the *NDVI* is estimated to be ~0.036 for bare sand and ~0.055 for cyanobacterium crust. Since the surface is mainly covered with biogenic crust on the Israeli side and bare sand on the Egyptian side, we use the *NDVI* of cyanobacteria crust as $NDVI_b$ for the Israeli subset and that of bare sand as $NDVI_b$ for the Egyptian subset. Atmospheric corrections were made to the images before computation of *NDVI* for vegetation analysis.

After the computation, we carried out three aspects of analysis: vegetation cover changes of cross-sections on both sides of the border, spatial variation of vegetation cover in the region, and seasonal vibration of average vegetation cover rates on the two sides.

4. Results and analysis

4.1. Results from the field observation

Direct sampling results from the field observation of the five rectangular plots are presented in Tables 1 and 2. The sizes of the plots range from 330 to 1330 m^2 (Table 1). Total sampling area of the five plots is 3851 m^2. As indicated in Table 2, no obvious differences in vegetation cover could be seen between the interdune valley and the dune slope. However, vegetation distribution was far from even in the region. The cover rate of vegetation tended to be different between the top dune and the dune slope or interdune. According to the measurement, average vegetation cover was ~15%, with interdune and dune slope 15–17% and top dune 10–11%. The biogenic crust surface accounted for over 2/3 of the total surface, while the bare sand made up ~15%. Although the observation was conducted at the Nizzana Research Site, the results are likely to be representative of the land cover structure on the Israeli side.

4.2. Results from the aerial photograph interpretation

Image statistics indicated that the Israeli subset has a total of 3,698,857 pixels and the Egyptian one 8,896,446. Pixels with DN values $\leqslant 60$ accounted for 17.4% in the Israeli subset and 6.4% in the Egyptian one. The ratio of the pixels to the total was 18.7% in the Israel subset and 6.9% in the Egypt one. This obvious difference in vegetation cover has a significant contribution to the sharp contrast of spectral reflectance in remote sensing images, as mentioned by Otterman (1974, 1977, 1981), Warren and Harrison (1984), Tsoar and Møller (1986), and Tsoar and Karnieli (1996).

We then measured the other three land cover patterns in the two subsets. Table 3 shows the measurement results in the Egypt subset. Large differences in vegetation cover can be seen among various CV (biogenic crust mixed with vegetation) plots, ranging from 5% to 16% (Table 3). The average vegetation cover rate was ~12% on CV plots and only 1.4% on PV (playa mixed with vegetation) plots. Five plots were sampled to compare vegetation cover changes on SV (bare sand mixed with vegetation) plots (Table 3), giving an average vegetation rate of 3.2%. According to these measurements, we obtained the following statistical results of land cover structure for the Egyptian subset: vegetation 568,946 pixels, accounting for 6.4% of the total; biogenic crust 2,426,254 pixels, accounting for 27.3%; playa 292,859 pixels, accounting for 3.3%, and bare sand 5608,387 pixels, accounting for 63.0% (Table 3).

As seen from Fig. 2, not only vegetation density, but also biogenic crust area on the Egyptian side decreased rapidly with distance from the border. Thus, it was necessary to determine vanishing rates of vegetation cover and biogenic crust surface. Sampling three strips with different distances from the border gave the results shown in Fig. 3. Opposite changes were observed between bare sand and biogenic crust. The two patterns had a cover rate very close to each other in strip 1 (close to the border): 43.6% for biogenic crust and 44.4% for bare sand. However, in strip 3 (furthest from border), the rate increased to ~73.4% for sand and drops to 18.0% for crust. Since the photograph only covered a small part of the Egyptian side, one could expect that the cover rate might be above 75% for sand and be below 15% for crust. Vegetation rate also decreased, but playa rate increased slowly with distance: from 9.4% through 5.6–4.8%, and from 2.5% through 3.5–3.7%,

Table 3
Vegetation cover changes in the Egyptian subset of aerial photograph

Plots	Total pixels	Vegetation (%)	Plots	Total pixels	Vegetation (%)
CV1	622,094	11.9	PV1	15,979	4.4
CV2	331,814	4.7	PV2	281,158	1.3
CV3	50,567	5.9	Total	297,136	1.4
CV4	957,241	15.9	SV1	489,405	3.7
CV5	156,766	14.8	SV2	243,333	4.8
CV6	532,890	10.8	SV3	268,000	2.5
CV7	110,809	9.2	SV4	213,043	4.6
Total	2,762,180	12.2	SV5	374,684	1.9
			Total	1,588,466	3.2

Note: CV denotes plot of biogenic crust mixed with vegetation, PV playa mixed with vegetation, and SV bare sand mixed with vegetation.

respectively (Fig. 3). Thus, the rate on average could be estimated as ~4.5% for vegetation and ~3.5% for playa.

Four sand dunes were distinguished on the Israeli subset, and Table 4 showed the results of the measurements made on them. Thus, we had 4,051,451 pixels of bare sand, accounting for 11.2% of the subset total. Several PV plots were available on the subset, with playa pixels accounting for 3.5% of the subset total. Vegetation cover rate in CV plots was also measured to determine their differences: average cover was 18.9% in the interdunes and 23.5% on the dune slopes. For the latter, the average rate was ~22.6% at the bottom and 24.9% in the middle. A higher vegetation rate on the dune slopes than in the interdunes might be attributed to water supply from the dune itself. Generally water also penetrates in horizontal direction in a sand dune. This means that there is likely to be a large supply of water in the dune slopes than in the interdunes, where water comes only from vertical direction or from deeper layers.

To compare the spatial distribution of vegetation in the Israeli subset, three sampling strips with different distances from the border were taken for measurement: giving a cover rate of 12.6% for strip 1 (close to the border), 15.8% for strip 2 (in the middle), and 17.7% for strip 3 (furthest from the border). Thus, vegetation density increases with distance from the border. Actually, due to the Israeli conservation policy, the sand dune region on the Israeli side has retained in its natural evolutionary status and is rarely disturbed by anthropogenic activities. With distance from the border, the effects of meteorological

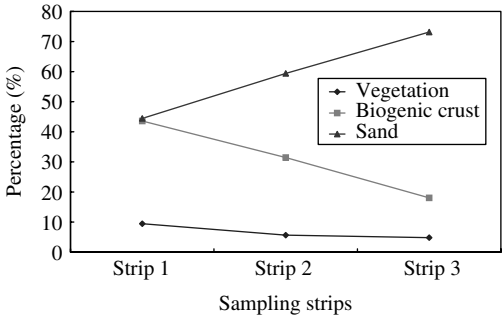

Fig. 3. Changes in land cover structure on the Egyptian subset of aerial photograph.

Table 4
Vegetation cover changes in the Israeli subset of aerial photograph

Plots	Total pixels	Vegetation (%)
SV1	714,146	3.0
SV2	1,067,436	2.7
SV3	994,024	13.2
SV4	815,270	9.0
SV5	753,858	5.1
Total	4,344,734	6.8

Note: SV denotes plot of bare sand mixed with vegetation.

factors from the nearby Egyptian side decrease, resulting in rampant vegetative growth in the region's inner areas.

4.3. Results from the Landsat TM and SPOT image analysis

Fig. 4 represents one of the results from the analysis of the TM and SPOT images. Three cross-sections paralleling the border were taken for comparison of vegetation cover changes on both sides. The changes shown in Fig. 4 were computed from the TM image acquired on March 29, 1995. Since March is the blooming season for desert plants in the arid region, the changes in Fig. 4 represent typical differences in vegetation cover across the border. The Israeli side is clearly seen to have a higher vegetation cover rate than the Egyptian side. Three cross-sections were taken along the northwest-to-southeast direction, and with cross-section 1 close to the border, 2 in the middle and 3 further away. To reveal the general trend of vegetation cover changes along the cross-sections, each was averaged from 4 nearby samplings. Despite the big vibration, four features can be identified in Fig. 4. First, vegetation rate in the northwest was generally higher than that in the southeast. For the Israeli cross-sections, the rate usually changed from 22–30% in the northwest to 12–20% in the southeast. For the Egyptian cross-sections, it changed from 5–12% in the northwest to 0–5% in the southeast. This can probably be attributed to distance from the Mediterranean Sea. The arid region depends mainly on the Mediterranean climate for rainfall. Within a short distance from the sea, sharp differences in rainfall magnitude can be found. Uneven distribution of rainfall in the region may shape impacts on spatial changes in vegetation cover density.

Second, vegetation cover rates in the cross-sections differed with distance from the border. On the Israeli side, the rates increased from 16.1% for cross-sections I1 (close to the border) through 17.2% for I2 (in the middle) to 19.5% for I3 (furthest from the border). Opposite changes were seen on the Egyptian side, changing from 5.4% for E1 (close to the border) through 5.0% for E2 (in the middle) to 3.3% for E3 (furthest from the border). Third, the Israeli side had a much higher average vegetation cover than the Egyptian side. The average for cross-sections I1, I2 and I3 was 17.6%, while that for E1,

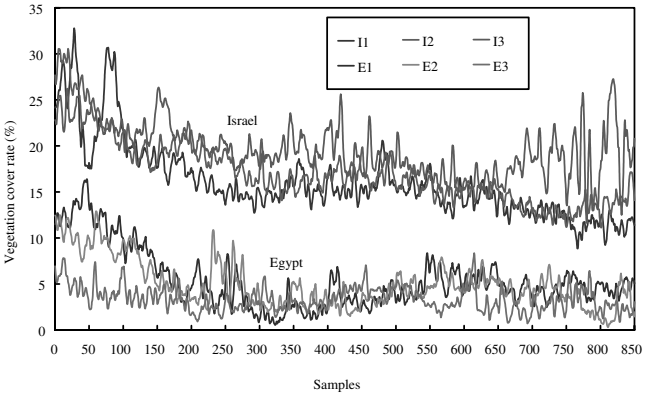

Fig. 4. Vegetation cover changes in cross-sections of the Israeli and the Egyptian sides. I1, I2 and I3 are cross-sections 1, 2, and3 on the Israeli side; E1, E2 and E3 are cross-sections 1, 2, and 3 on the Egyptian sides. Cross-section 1 is close to the border, 2 in the middle, and 3 furthest from the border.

E2 and E3 was only 4.6%. This may represents the actual difference in vegetation cover across the border. Finally, spatial distribution of vegetation cover was far from even on both sides. Great vibration was a common feature to the cross-sections from both sides, particularly I3 and E3.

Fig. 5 highlights the detailed spatial variations in vegetation cover of the region. In addition to the obvious differences across the border, the upper part of the Israeli side had higher vegetation cover than the lower part. Vegetation cover rate was generally up to 20–30% in the upper part, whereas it was only 12–20% in the lower part. The wadi near the Nizzana Research Site also had remarkably dense vegetation covering its bed. In the lower right were the small hills, where relatively higher vegetation cover was also seen in the valleys, due to more water available.

Table 5 and Fig. 6 compare vegetation cover changes in various seasons, computed from the available 6 Landsat TM images of the region. Seasonal changes of vegetation cover in the arid region depend strongly on rainfall. The climate in the region follows a typical Mediterranean pattern, with the rainy season generally starting in November and ending in April, despite large annual vibrations. Therefore, the period from January to March is usually the best growing season for green plants in the region. This is why we obtained much higher average vegetation cover rates in TM images 19870404, 19950124 and 19950329. During the dry season (generally from May to October), the desert plants gradually go into dormancy, due to a lack of water. The plant canopy is reduced to minimum in order to minimize water loss through evapo-transpiration. Table 5 indicates that seasonal changes in vegetation cover on the Israeli side may be from above 18% in the growing season to ~5% in the dry season. On the Egyptian side, the rate may be ~5% in the growing season, while it may drop to below 2% in the dry season.

Seasonal changes of vegetation cover in the region are more clearly seen from the lower and left parts of Table 5, which were computed from 20 SPOT images of the region around

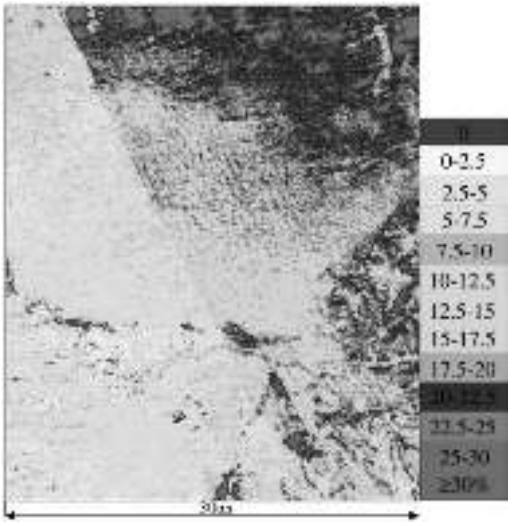

Fig. 5. Vegetation cover rate of the Israel–Egypt border region, retrieved from Land TM image of March 29, 1995.

Table 5
Changes in average vegetation cover rates on both sides of the border in the arid region

Imaging dates	No.	Israel (%)	Egypt (%)	Imaging dates	No.	Israel (%)	Egypt (%)
Landsat TM images				*SPOT images*			
19870404	1	16.5	4.2	20020116	7	8.7	3.9
19941121	2	7.5	1.7	20020131	8	10.4	4.4
19950124	3	16.3	4.5	20020304	9	16.9	4.9
19950329	4	18.7	4.8	20020416	10	9.0	3.3
19950617	5	10.3	3.6	20020425	11	7.2	2.6
19950921	6	8.3	3.2	20020521	12	6.2	2.9
				20021013	13	4.0	2.6
SPOT images				20021115	14	8.6	2.9
20010429	1	6.9	3.5	20021206	15	9.7	3.5
20011123	2	4.8	2.7	20021215	16	10.5	3.8
20011125	3	4.1	2.5	20021230	17	13.8	4.3
20011202	4	5.9	3.1	20030110	18	14.4	4.6
20011216	5	6.1	3.4	20030201	19	16.9	4.9
20011227	6	6.6	3.5	20030227	20	18.2	5.3

Note: Imaging date is in the format of yyyymmdd. For example, imaging date 20030227 refers to February 27, 2003.

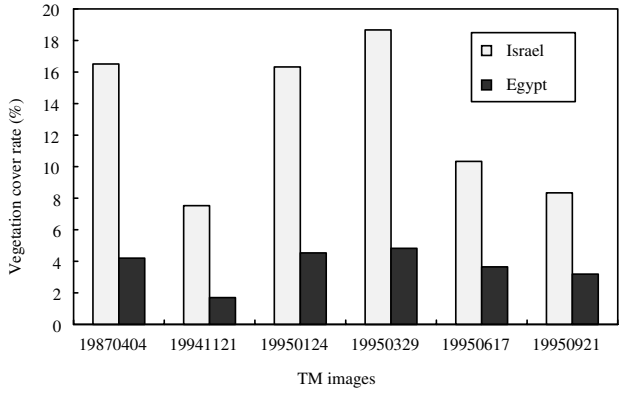

Fig. 6. Vegetation cover changes of the arid region across the Israel–Egypt border, estimated from Landsat TM images, which are named using imaging date in a format of yyyymmdd, for example 19950921 referring to imaging date of September 21, 1995.

the Nizzana Research Site. A comparison of vegetation cover rates on both sides is presented in Figs. 7 and 8. Spatial variation is clearly seen across the border on the SPOT image (Fig. 7) acquired on February 1, 2003. Since the imaging date was during the growing season, vegetation cover rate shown in Fig. 7 reflects the region's maximal status. The rate on the Israeli side is high up to 22–30% in the dunes near the wadi. In contrast, the Egyptian side generally has a rate of below 7% (Fig. 7) and dense vegetation can only be seen along the wadi bed, indicating that the Egyptian side is dominated by bare sand surface. Fig. 8 highlights the seasonal changes in vegetation cover, where they are seen to be similar to those from Landsat TM images. The highest vegetation cover rates are seen in the SPOT images 9, 19 and 20, acquired during the growing season.

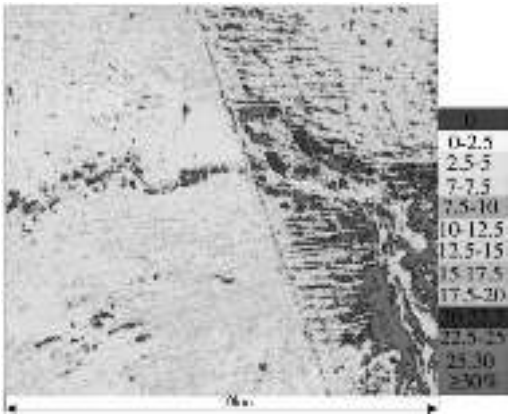

Fig. 7. Vegetation cover rate of the Israel–Egypt border region, retrieved from SPOT image of February 1, 2003. Geographic location of the image is boxed in Fig. 1.

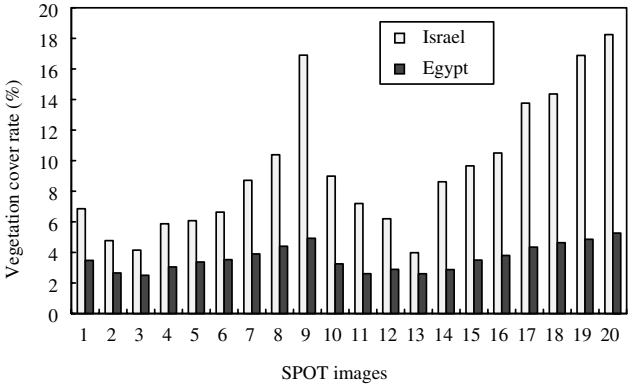

Fig. 8. Vegetation cover changes of the arid region across the Israel–Egypt border, estimated from SPOT images. Refer to Table 5 for imaging dates.

5. Conclusion

Three methods were employed in this study to estimate land cover structure in the arid region across the Israel–Egypt border. Field observation at the Nizzana Research Site of Israel indicated that, on average, vegetation covers ~15.6% of the ground, biogenic crust 69.4%, bare sand 11.9% and playa 3.0%. Results from measurements made on the aerial photograph supported the existence of a sharp difference in land cover structure across the border. Vegetation covered ~17.4% on the Israel subset and 6.4% on the Egypt one. Biogenic crust occupied ~67.9% on the Israel subset and 27.3% on the Egypt one. Bare sand covers ~11.2% on the former and 63.6% on the latter. Playa only covered a small percentage: 3.5% and 3.3% on the Israeli and Egyptian subsets, respectively.

Analysis of vegetation cover on the available TM and SPOT images strongly supported the results from the aerial photograph interpretation. Cross-section analysis revealed four features of vegetation cover changes in the region: the cover rate was obviously higher on

the Israeli side than on the Egyptian side. During the growing season, e.g. in March, the rate was above 17.6% on the Israeli side and 4.6% on the Egyptian side. Vegetation density generally decreased with distance from the Mediterranean Sea. Opposite changes in vegetation cover occurred between the two sides with respect to distance from the border: on the Israeli side, vegetation cover rate showed an increasing trend with the distance; this is in contrast to its slight decreasing trend with distance on the Egyptian side (Fig. 4). Finally vegetation density is far from even in terms of spatial distribution.

Time series analysis of the TM and SPOT images highlighted a remarkable change of vegetation cover in different seasons. Generally speaking, average vegetation cover rate on the Israeli side can reach over 18% in the growing season, whereas it can drop to below 5% in the dry months. On the Egyptian side, the rate may increase to ~5% in the growing season and drop to below 2% in the dry months. Since the surface of the Israeli side is mainly biogenic crust under canopy, and that of the Egyptian side is mainly bare sand, it is expected that the cover rate of biogenic crust on the Israeli side will change from 70% in the wet season to as high as 84% in the dry months. The rate of bare sand on the Egyptian side may range from ~80% in the wet season to 82% in the dry months.

Therefore, it is reasonable to estimate the land cover structure of the region as follows. During the growing season, average vegetation cover rate may rise to above18% on the Israeli side and over 5% on the Egyptian side. However, the rate in the dry season may drop to below 5% on the Israeli side and 2% on the Egyptian side. This indicates a very high vibration in seasonal changes of vegetation cover in the region. Accordingly, biogenic crust occupies 71–84% of the surface on the Israeli side from the wet to dry seasons, and 12% on the Egyptian side. Bare sand covers 7.5% on the Israeli side and 79–82% on the Egyptian side. Playa accounts for 3.5% on both sides. This estimate of land cover structure has successfully used to model and explain the land surface temperature difference across the border (Qin et al., 2002b, 2005).

Acknowledgement

This work was supported by China National Natural Science Foundation projects (No: 30571078 and 40471096). The authors sincerely thank the following people for their assistance: Dr. Heike Schmid, our colleague at the Remote Sensing Laboratory, for helping to access the region for ground truth measurements; Mr. Simon Berkowics, administrator of The Arid Ecosystems Research Center, Inst. of Earth Sciences, The Hebrew University of Jerusalem, for giving us permission to conduct ground truth measurements at the Nizzana Research Site; Dr. Dan Blumberg, Dr. Haim Tsoar, Mr. Gil Revivo, Dr. Robi Stark and Mr. Guy Serbin from Ben Gurion University of the Negev for personal communications about the region.

References

Bahre, C.J., Bradbury, D.E., 1978. Vegetation change along the Arizona–Sonora boundary. Annals of the Association of American Geographers 68, 145–165.

Balling Jr., R.C., 1989. The impact of summer rainfall on the temperature gradient along the United States–Mexico border. Journal of Applied Climatology 28, 304–308.

Balling Jr., R.C., Klopatek, J.M., Hildebrandt, M.L., Moritz, C.K., Watts, C.J., 1998. Impacts of land degradation on historical temperature records from the Sonoran desert. Climatic Change 40, 669–681.

Cihlar, J., 2000. Land cover mapping of large areas from satellites: status and research priorities. International Journal of Remote Sensing 21, 1093–1114.

Danin, A., 1991. Plant adaptation in desert dunes. Journal of Arid Environment 21, 193–212.

Gerson, R., Amit, R., Grossman, S., 1985. Dust Availability in Desert Terrains: A Study in the Deserts of Israel and the Sinai. The Hebrew University of Jerusalem, Israel 169pp.

Karnieli, A., 1997. Development and implementation of spectral crust index over dune sands. International Journal of Remote Sensing 18, 1207–1220.

Karnieli, A., Tsoar, H., 1995. Spectral reflectance of biogenic crust developed on desert dune sand along the Israel–Egypt border. International Journal of Remote Sensing 16, 369–374.

Kerr, Y.H., Lagouarde, J.P., Imbernon, J., 1992. Accurate land surface temperature retrieval from AVHRR data with use of an improved split window algorithm. Remote Sensing Environment 41, 197–209.

Kidron, G.J., Yair, A., 1997. Rainfall-runoff relationship over encrusted dune surfaces, Nizzana, Western Negev, Israel. Earth Surface Processes and Landforms 22, 1169–1184.

Otterman, J., 1974. Baring high-albedo soils by overgrazing: a hypothesized desertification mechanism. Science 186, 531–533.

Otterman, J., 1977. Anthropogenic impact on the surface at the Earth. Climatic Change 1, 137–155.

Otterman, J., 1981. Satellite and field studies of man's impact on the surface in arid regions. Tellus 33, 68–77.

Otterman, J., Robinove, C.J., 1982. Landsat monitoring of desert vegetation growth in 1972–1979 using a plant shadowing model. Advance of Space Researches 2, 45–50.

Otterman, J., Tucker, C.J., 1985. Satellite measurements of surface albedo in semi desert. Journal of Climate and Applied Meteorology 24, 228–235.

Pinker, R.T., Karnieli, A., 1995. Characteristic spectral reflectance of a semi-arid environment. International Journal of Remote Sensing 16, 1341–1363.

Qin, Z., Karnieli, A., Berliner, P., 2001. Thermal variation in the Israel–Sinai (Egypt) peninsula region. International Journal of Remote Sensing 22, 915–919.

Qin, Z., Karnieli, A., Berliner, P., 2002a. Remote sensing analysis of the land surface temperature anomaly in the sand dune region across the Israel–Egypt border. International Journal of Remote Sensing 23 (19), 3991–4018.

Qin, Z., Berliner, P., Karnieli, A., 2002b. Micrometeorological modeling to understand the thermal anomaly in the sand dunes across the Israel–Egypt border. Journal of Arid Environment 51 (2), 281–318.

Qin, Z., Berliner, P., Karnieli, A., 2002c. Numerical solution of a complete surface energy balance model for simulation of heat fluxes and surface temperature under bare soil environment. Applied Mathematics and Computation 130 (1), 171–200.

Qin, Z., Karnieli, A., Berliner, P., 2005. Ground temperature measurement and emissivity determination to understand the thermal anomaly and its significance on arid ecosystem development in the sand dunes across the Israel–Egypt border. Journal of Arid Environment 60 (1), 27–52.

Tielböger, K., 1997. The vegetation of linear desert dunes in the northwestern Negev, Israel. Flora 192, 261–278.

Tsoar, H., Karnieli, A., 1996. What determines the spectral reflectance of the Negev-Sinai sand dunes. International Journal of Remote Sensing 17, 3513–3525.

Tsoar, H., Møller, J.T., 1986. The role of vegetation in the formation of linear sand dunes. In: Nickling, W.P. (Ed.), Aeolian Geomorphology. Allen & Unwin Inc., Boston, USA, pp. 75–95.

Warren, A., Harrison, C.M., 1984. People and the ecosystem: biogeography as a study of ecology and culture. Geoforum 15, 365–381.